

Three-Component Coupling Reaction

N-Heterocyclic Carbene-Protected Ag Nanoparticles Immobilized on Polyacrylonitrile Fiber as Efficient Catalysts for a Three-Component Coupling Reaction

Jian Cao and Hongqi Tian*^[a]

Abstract: Metal nanoparticles (NPs) are routinely stabilized by the introduction of capping agents or their distribution on supports. In this context, we report the preparation and characterization of N-heterocyclic carbene (NHC)-stabilized silver NPs supported on polyacrylonitrile fiber (PANF). As a result, Ag loadings of up to 8% and particle sizes of 11.0 ± 3.2 nm were achieved. This novel nanocomposite catalyst demonstrated high activity in addition to excellent stability and reusability in the three-component reaction between alkynes, haloalkanes, and amines. In this system, the AgNPs

were stabilized by both a support effect and a ligand effect. The unique NHC-protected AgNP structure and the PANF support provide a synergistic effect in the deprotonation of $C_{sp}-H$ bonds, with turnover numbers of up to 3500. This catalyst was successfully recycled over eight runs without any significant loss in activity, and with no significant aggregation of the AgNPs. Moreover, implementation of a flow system with PANF-NHC@Ag as catalyst leads to an efficient productivity of 57 mmol h^{-1} .

Introduction

Metal nanoparticles (NPs) have attracted growing attention in recent years owing to their unique properties compared with those of their bulk counterparts.^[1] These properties have resulted in the application of NPs in a range of fields, including drug research,^[2] sensors,^[3] and catalysis.^[4,5] As such, the successful preparation of metal NPs with small diameters is critical for enhancing catalytic performances owing to the high degree of dispersion and the nanosize effect of small particles.^[6] The stabilization of such metal NPs is therefore essential, and this is commonly achieved by the introduction of capping agents^[7] or by distribution of the metal NPs/clusters on supports.^[4]

To date, a wide range of capping agents have been reported for the stabilization of metal NPs, with examples including thiols, amines, disulfides, phosphines, and N-heterocyclic carbenes (NHCs).^[7–10] More specifically, the formation of coordination bonds between neutral and electron-rich NHCs and the surfaces of metal NPs is crucial, as it allows the NPs to retain their unique nanoscale properties.^[11] In 2010, Ranganath et al. reported a heterogeneous NHC-modified $Fe_3O_4/PdNPs$ cata-

lyst.^[12] This novel NP catalyst efficiently catalyzed asymmetric α -arylation reactions with up to 85% ee. Furthermore, Salorinne et al. described a bottom-up approach for the synthesis of novel NHC-protected AuNPs by employing water-soluble and pH-tunable NHCs,^[13] whereas Ferry et al. employed bidentate hybrid NHC–thioether ligands to stabilize Pd and AuNPs for use in various catalytic transformations.^[14] However, despite huge advances in this area, only a few examples of supported NHC-NP systems have been reported, with one example including an extensive characterization of an NHC-modified supported heterogeneous Ru/K- Al_2O_3 catalyst. The tunability of Ru/K- Al_2O_3 by NHCs played an important role in a perfectly chemoselective hydrogenation.^[15]

In the context of NPs, AgNPs are one of the most frequently employed nanostructures, and have been used in a multitude of applications, including catalysis, imaging, drug delivery, and theragnostics.^[16–18] However, only a few examples of NHC-functionalized AgNPs have been described in the literature. For example, in 2012, Yu et al. reported the stabilization of a AgNP catalyst by a NHC polymer.^[19] This novel nanoscale catalyst exhibited an excellent activity in addition to good stability and reusability for the carboxylation of terminal alkynes with CO_2 at room temperature. These results therefore indicate that the preparation of novel NHC-functionalized AgNPs could be of particular importance in the context of nanochemistry.

In general, NPs exhibit higher catalytic activities than their bulk counterparts. However, owing to their reduced thermodynamic stabilities,^[1] modifications such as the addition of ligands and capping agents or the formation of core–shell type particles have been examined to produce stable particles.^[9] Unfortunately, the application of these modified catalysts often

[a] Dr. J. Cao, Prof. H. Tian

Tianjin Key Laboratory of Radiation Medicine and Molecular Nuclear Medicine, Institute of Radiation Medicine
Chinese Academy of Medical Science and Peking Union Medical College,
Tianjin 300192 (China)
E-mail: tianhongqi@irm-cams.ac.cn

 Supporting information and the ORCID identification number(s) for the author(s) of this article can be found under:
<https://doi.org/10.1002/asia.201800154>.

results in facile NP aggregation and the formation of a deactivated bulk mass, which in turn leads to poor activities and re-usabilities. To address this issue, a combination of supports and NPs may be considered a promising way forward. Indeed, the ease of separation, the simple regeneration, and the high stabilities of supported catalysts have spurred the development of heterogeneous nanocatalysis, in addition to the direct utilization of such catalysts in continuous-flow processes.^[1,4,5] To date, various support materials have been employed as templates in the manufacture of metal NPs owing to the beneficial synergistic properties of nanometal/polymer composites. For example, Emam et al. reported a simple, green, and inexpensive one-pot method for the preparation of AgNPs, AuNPs, and Ag-Au nano-alloys on a cellulosic solid support. In this case, immobilization of the NP/bimetallic nanostructures produced a catalyst for the reduction of *p*-nitroaniline.^[20] Furthermore, Liu et al. employed mesoporous SBA-15-supported AgNPs as a catalyst system for an A3 coupling reaction.^[21]

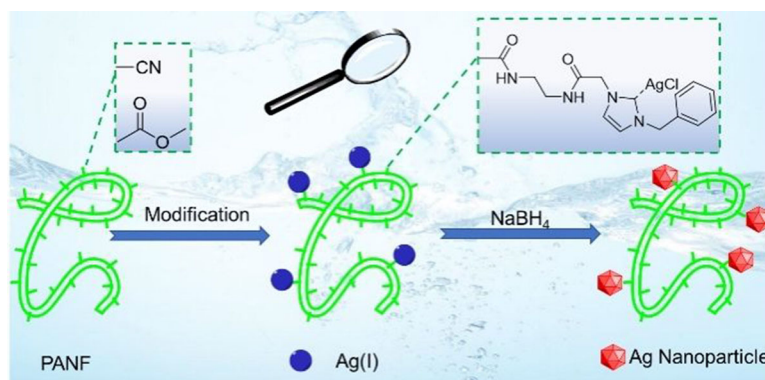
Recently, the use of fibers such as polyacrylonitrile fiber (PANF), polypropylene fiber, and cotton fiber as support materials for adsorbents, metal ion sensors, and catalysts has been reported.^[22–27] Indeed, PANF is a particularly promising support material owing to its inexpensive source, porous structure, and good stability. Moreover, the PANF framework contains an abundance of -CN groups, which can be easily functionalized and immobilized with various moieties.^[25,27] For example, previous studies have reported the immobilization of Ag complexes to afford PANF-supported Ag complexes.^[27] Thus, we herein report a novel strategy for the synthesis of a sequence of PANF-supported Ag nanoparticles (PANF-NHC@Ag) based on the use of NaBH₄ to reduce PANF-supported NHC-Ag complexes (Scheme 1). The resulting PANF-NHC@Ag materials will then be characterized, and their catalytic performances in the three-component reaction between aldehydes, halomethanes, and alkynes (AHA coupling) will be evaluated. This transformation is of particular interest, as the AHA coupling reaction is an important approach in the synthesis of propargylamines, which are recurrent moieties in biologically active compounds and are also valuable intermediates in organic synthesis.^[28–30]

Results and Discussion

Preparation and characterization of the fiber-supported AgNPs

As outlined in Scheme 1, the preparation of PANF-NHC@Ag was based on the reduction of a PANF-supported NHC-Ag complex (PANF-NHC-Ag) by using NaBH₄.^[13] The first step in this synthetic route involved the modification of PANF to give the supported Ag complexes.^[27] This was followed by reduction of the Ag complexes to yield the desired fiber-supported AgNPs. To investigate the influence of the ligand, aminated PANF coordinated with AgNO₃ was also used as a precursor, which was later reduced to produce amino-protected NPs (PANF-Am@Ag). A detailed typical procedure for the preparation of these catalysts is given in the Supporting Information.

Following the successful preparation of PANF-NHC-Ag, the extent of its modification was measured by calculating the weight gain and by determining the concentration of metal ions by inductively coupled plasma optical emission spectroscopy (ICP-OES; Table S1 in the Supporting Information).^[27] The obtained PANF-NHC-Ag was then reduced, and the NP size was controlled by tuning the reduction time and functionality of PANF-NHC-Ag. To investigate the unique and attractive features of the prepared NPs, transmission electron microscopy (TEM) was employed to characterize the nanoscale structures (see Figure 1). As shown in Figure 1a, nano-sized spherical Ag particles with average diameters of 11.0 ± 3.2 nm were successfully prepared and immobilized on the fiber surface. Upon tuning the reduction time and the functionality (*F*), the NP size could be varied from 11.0 nm (4–18 nm) to 44.5 nm (24–52 nm; Figure 1). As indicated, upon increasing the functionality of the precursor, the formation of Ag clusters was promoted, with aggregation of the AgNPs being observed at higher loadings. In addition, increased reduction times resulted in NP aggregation (Figure 2). Under optimized conditions, AgNPs with a loading of 8% (0.75 mmol g⁻¹) and an average diameter of 11.0 ± 3.2 nm were successfully prepared. However, upon examination of the obtained PANF-Am@Ag by TEM (Figure S1 in the Supporting Information), few NPs were detected, thereby demonstrating the importance of the NHC in stabilizing the



Scheme 1. Schematic illustration of the preparation of PANF-supported AgNP catalysts.

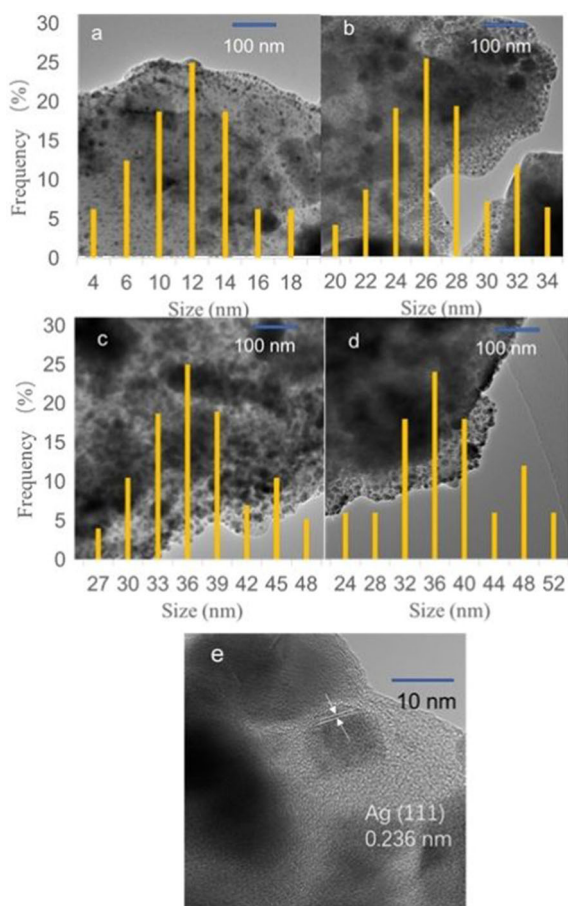


Figure 1. Typical TEM images of PANF-NHC@Ag: (a) $F = 0.75 \text{ mmol g}^{-1}$, reduction for 6 h; (b) $F = 0.75 \text{ mmol g}^{-1}$, reduction for 12 h; (c) $F = 1.1 \text{ mmol g}^{-1}$, reduction for 6 h; (d) $F = 1.1 \text{ mmol g}^{-1}$, reduction for 12 h; and (e) $F = 0.75 \text{ mmol g}^{-1}$, reduction for 6 h.

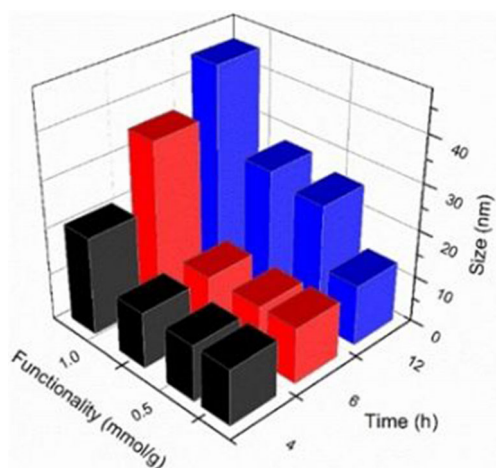


Figure 2. Control of NP size by tuning the reduction time and functionality of PANF-NHC-Ag.

AgNPs. Furthermore, the high-resolution transmission electron microscopy (HRTEM) image of PANF-NHC@Ag is shown in Figure 1e, where lattice fringes with spacings of approximately

0.24 nm can be clearly observed, which can be attributed to the lattice spacings of the (111) planes of the AgNPs.^[31]

The modified fibers were then analyzed by scanning electron microscopy (SEM) to examine both the general morphology and the microscopic fine structure. As shown in Figure 3,

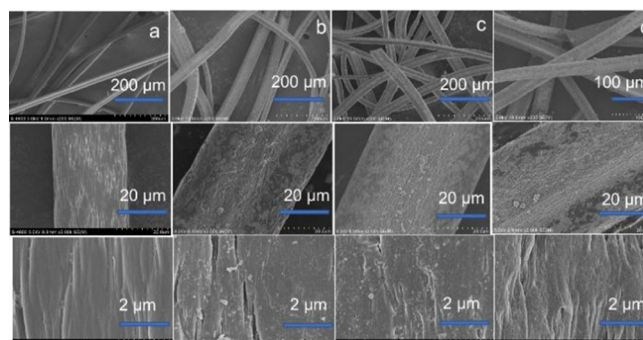


Figure 3. Scanning electron microscopy: (a) PANF; (b) PANF-Am@Ag; (c) PANF-NHC@Ag; and (d) PANF-NHC@Ag after eight catalytic runs.

the prepared PANF-NHC@Ag and PANF-Am@Ag exhibited greater thicknesses and surface coarseness than PANF itself. In addition, following reduction by NaBH_4 , Ag nanoparticles were found on the PANF-NHC@Ag surface. Subsequently, energy dispersive spectroscopy (EDS) was utilized to characterize the PANF-NHC@Ag catalyst. As shown in Figure 4a, peaks corresponding to C, N, O, and Ag were observed in the EDS spectrum, thereby confirming that the AgNPs were immobilized on the fiber surface. In addition, examination of the prepared PANF-NHC@Ag by energy-dispersive X-ray elemental mapping (Figures 4b–g) showed the highly dispersed AgNPs in the PANF matrix as bright spots. The dispersion of N, C, and O over the fiber surface was also confirmed by elemental mapping.

Analysis of the original PANF by X-ray diffraction (XRD, Figure 5a) showed an intense reflection peak at $2\theta = 17^\circ$ attributed to the (100) diffraction of the hexagonal lattice, which is constructed through the parallel tight packing of the molecular rods. This confirms that intermolecular repulsions between the CN groups of PANF result in the formation of a rod-like conformation.^[32] In the case of PANF-NHC@Ag (Figure 5c), four additional peaks at $2\theta = 38.5, 44.3, 64.5,$ and 77.1° were ascribed to the (111), (200), (220), and (311) planes, respectively,^[21] which correspond to the face-centered cubic (fcc) structure of the AgNPs (JCPDS No. 00-004-0783). This result therefore confirms that Ag complexes were successfully transformed into AgNPs through reduction by using NaBH_4 , and that these NPs were subsequently deposited on the PANF surface.

X-ray photoelectron spectroscopy (XPS) was then utilized to examine both the chelating mechanism and the elemental composition. The full survey spectrum of PANF-NHC@Ag (Figure 6a) shows principal energy levels for O 1s, N 1s, Ag 3d, and C 1s at 536.10, 403.26, 374.02, 368.03, and 287.34 eV.^[31] In addition, the high-resolution XPS spectrum (Figure 6b) shows the typical doublet (resulting from spin-orbital splitting) for an electron on a 3d level of Ag. Furthermore, the high-resolution

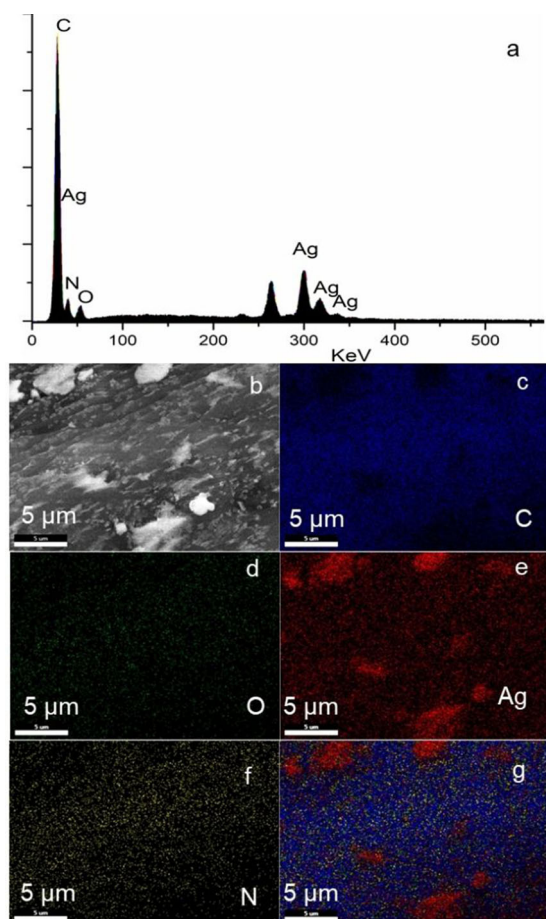


Figure 4. (a) EDS spectrum for PANF-NHC@Ag, (b) SEM image, and (c)–(g) energy-dispersive X-ray elemental mapping images for PANF-NHC@Ag.

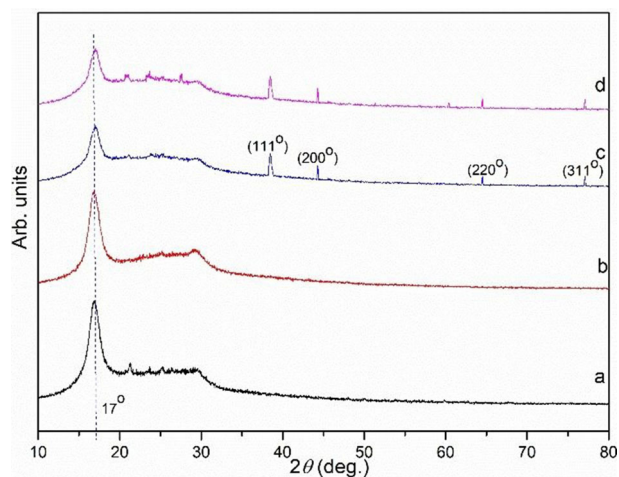


Figure 5. XRD patterns of the fiber samples: (a) PANF; (b) PANF-NHC-Ag; (c) PANF-NHC@Ag; and (d) PANF-NHC@Ag, after eight catalytic runs.

Ag XPS spectrum of PANF-NHC-Ag contained two peaks at 368.35 and 374.28 eV (Figure 6b-I), which corresponded to $\text{Ag}3\text{d}_{3/2}$ and $3\text{d}_{5/2}$, respectively, and which can be attributed to the NHC-Ag complex.^[33] Following reduction, the high-resolution Ag XPS spectrum of PANF-NHC@Ag contained two peaks

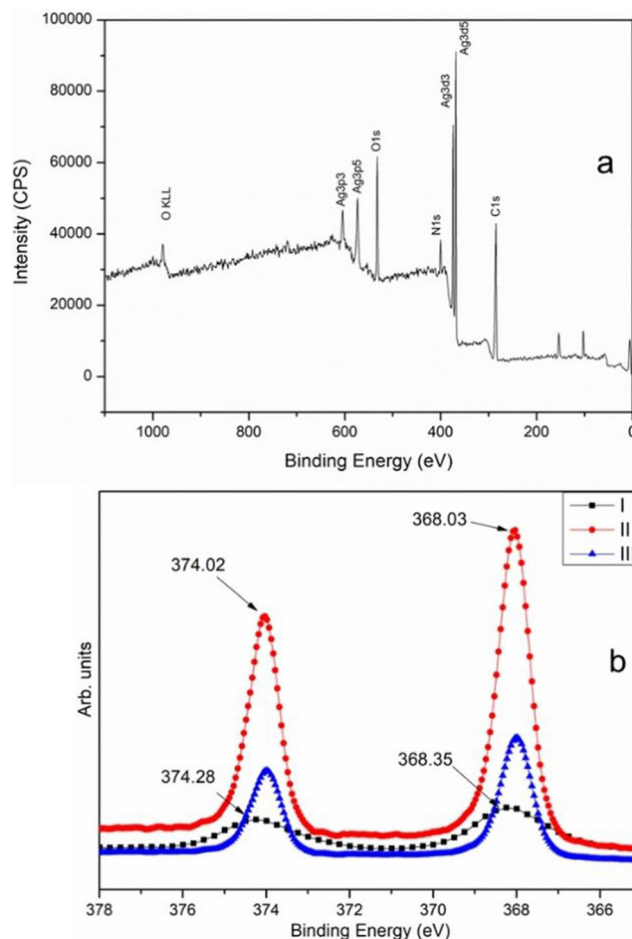


Figure 6. XPS spectra: (a) survey scan of PANF-NHC@Ag, and (b) high-resolution XPS narrow scan of Ag 3d (I, PANF-NHC-Ag; II, PANF-NHC@Ag; III, PANF-NHC@Ag after eight runs).

at 368.03 and 374.02 eV (Figure 6b-II), which corresponded to $\text{Ag}3\text{d}_{3/2}$ and $3\text{d}_{5/2}$, respectively, and were attributed to the Ag nanoparticles.^[31] The Ag 3d peak for the recycled supported NPs is also shown (Figure 6b-III), which demonstrates that Ag^0 was the dominant form of Ag following catalyst recycling.

Solid-state ^{13}C NMR spectroscopy (Figure 7) was employed to confirm the proposed PANF framework and the incorporation of the NHC moiety. As indicated, the pure PANF material produced signals at 29.7, 122.1, and 172.5 ppm corresponding to the backbone carbon atoms, the cyano carbon atoms, and the ester carbonyl carbon atoms (Figure 7a).^[34,35] As expected, following amination, the signal corresponding to the ester carbonyl carbon atom disappears, and a new signal originating from the amide carbon atom appears at approximately 174.5 ppm. In addition, strong carbon signals corresponding to the NHC moieties can be seen at 137.0 and 130.1 ppm (Figure 7d), with long reduction times leading to the disappearance of the NHC structure (Figure 7c). As the NHC moiety stabilizes the NPs, longer reduction times result in the formation of bigger particles through aggregation (Figure 2).

The utilization of porous materials as the NP support also allows the generation of specific adsorption sites for reaction substrates.^[4] Thus, nitrogen adsorption/desorption isotherms

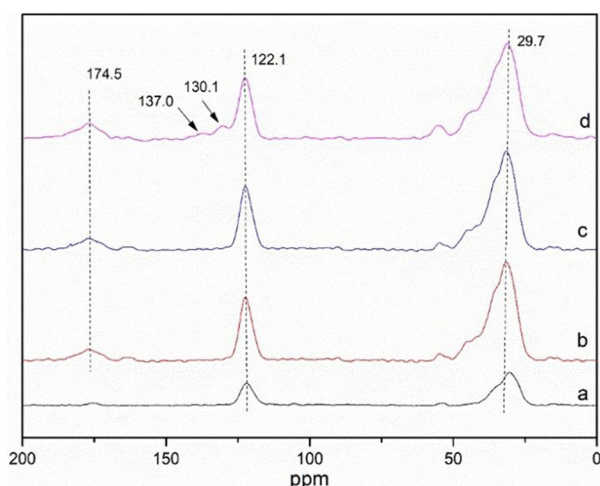


Figure 7. Solid-state ^{13}C NMR spectra for (a) PANF, (b) PANF-Am@Ag, (c) PANF-NHC@Ag following a long reduction time, and (d) PANF-NHC@Ag.

were performed on PANF before and after modification to characterize its porosity and surface area (see Table S2 in the Supporting Information). Following the grafting of ethylenediamine, the PANF surface area decreased to $33.1\text{ m}^2\text{ g}^{-1}$. In contrast, upon grafting of the NHC derivatives, the surface area increased to $55.1\text{ m}^2\text{ g}^{-1}$, with subsequent chemical reduction giving a further increase to $73.4\text{ m}^2\text{ g}^{-1}$ owing to the formation of AgNPs. As nanoscale pores were observed for the modified fibers, the porous materials were utilized as a NP support containing specific adsorption and active sites.

The detailed nucleation process for the formation of NPs from reaction solutions has been previously described by a two-step model.^[36] More specifically, the formation of NPs can be considered as a chemical reaction that produces solid AgNPs from solvated Ag^0 precursor atoms. As such, the individual nucleation and growth steps can be adapted and designed by tuning the concentration of Ag^0 , thereby allowing a controlled synthesis of AgNPs through application of the appropriate parameters (Figure 2). Indeed, a number of studies have reported that the nucleation process is critical in improving the catalytic performance of NPs.^[2] In the case of our system, nucleation occurs on the PANF surface. As the precursor PANF-NHC-Ag is hydrophilic, it is easily reduced to Ag^0 by NaBH_4 ,^[17] whereas the NHC moiety stabilizes the AgNPs owing to its electron-donating properties.^[7,9] Moreover, in the nucleation stage, Ag^0 aggregates with other Ag^0 atoms in close proximity owing to its immobilization on the PANF framework.

Catalytic activity of the supported catalysts in the three-component coupling reaction

The formation of C–C bonds by the deprotonation of $\text{C}_{\text{sp}}\text{--H}$ is one of the most versatile and graceful manipulations in organic chemistry. In this context, in 2010, an Au-catalyzed AHA coupling reaction was reported by Aguilar et al. for the efficient synthesis of propargylamines.^[37] In this reaction, the $\text{C}_{\text{sp}}\text{--H}$ and C–halogen bonds are activated by AuNPs to form new C–C and C–N bonds. Later, copper salts,^[38–41] In_2O_3 NPs,^[42] Fe^{III} ,^[43]

cobalt,^[44] Ag^{I} ,^[45] and AuNPs^[46] were also employed as catalysts in the AHA coupling reaction. In addition, the deprotonation of $\text{C}_{\text{sp}}\text{--H}$ bonds by AgNPs has been reported.^[19,47] However, the development of a new highly efficient and environmentally friendly AgNP catalytic system for the AHA coupling reaction is still desirable.

Thus, we initially investigated the catalytic performance of PANF-NHC@Ag in the AHA coupling reaction, by employing dichloromethane, phenylacetylene, and pyrrolidine as the model reactants. Optimization of the feed ratio for the terminal alkyne, dihalomethane, and amine components gave a ratio of 1.0:1.2:1.2. Typically, enhanced activities were found for organic bases such as triethylamine and 1,8-diazabicyclo[5.4.0]undec-7-ene (DBU), likely owing to their superior solubility over inorganic bases in this AHA coupling reaction (Table S3 in the Supporting Information). We also performed the coupling reaction by using Na_2CO_3 , NaHCO_3 , and Cs_2CO_3 , and yields in the range 70–82% were obtained in the presence of these inorganic bases (Table S3 in the Supporting Information, entries 3–5). In addition, this novel system typically yielded good performances in a range of common organic solvents. More specifically, the highest propargylamine yield was obtained in toluene, whereas other solvents, such as dimethyl sulfoxide, tetrahydrofuran, CH_3CN , and CH_2Cl_2 , afforded moderate to good yields (Table S3 in the Supporting Information, entries 6–9). Interestingly, in the absence of solvent, PANF-NHC@Ag gave an excellent yield of 86% (Table S3 in the Supporting Information, entry 10). As sustainability is a significant concern in the chemical industry, the neat reaction is preferable, as it allows the assembly of complex compounds without the requirement for solvents. Furthermore, the reported AgNP-catalyzed reaction was carried out smoothly at 25°C , and proceeded at lower temperatures compared with previously reported AHA reactions.^[45,46,48]

With the optimized conditions in hand, the substrate scope of the AHA coupling reaction was investigated (Table 1). Dichloromethane, dibromomethane, diiodomethane, and dibromomethylbenzene all produced good results (Table S3 in the Supporting Information, entries 11 and 12, and Table 1, **4b**), and excellent yields were achieved when using cyclic, heterocyclic, and acyclic aliphatic amines as the substrates (Table 1, **4a**, **4l**, and **4d**). Interestingly, AHA coupling products were also isolated when primary amines were used as substrates (Table 1, **4m** and **4n**).

To investigate the leaching of AgNPs, a filtration experiment was carried out to determine whether the AHA reaction was catalyzed in a heterogeneous or homogeneous manner.^[49] After allowing the reaction to proceed for 0.5 h, the PANF-NHC@Ag catalyst was removed from the reaction mixture by filtration. The reaction mixture was then allowed to stir for a further 1.5 h in the absence of the fiber catalyst, but no further increase in conversion was observed. In addition, the Ag content in the clear filtrate was < 1.0 ppm (as determined by ICP-OES), which confirms the stability of the supported catalyst.

The recyclability of the PANF-NHC@Ag catalyst was then investigated. Following the recovery of PANF-NHC@Ag from the reaction mixture by filtration, it was reused in the subsequent

Table 1. Three-component coupling reactions catalyzed by PANF-NHC@Ag.^[a]

	86% ^b		85% ^c		72% ^b		76% ^b
	80% ^c		85% ^b		80% ^b		82% ^c
	84% ^c		75% ^b		85% ^b		80% ^b
	80% ^c		81% ^b		83% ^b		

[a] Reaction conditions: haloalkanes (1.2 mmol), amines (1.2 mmol), alkynes (1.0 mmol), PANF-NHC@Ag (1 mol%, calculated based on Ag), DBU (2.0 mmol), 25 °C. [b] X = Cl. [c] X = Br.

run for the synthesis of **4a**. After eight consecutive cycles, the yield of **4a** was maintained at 81% (Figure 8a). The catalyst recyclability in the reactions employing CH₂Br₂ and dibromomethylbenzene as substrates was also investigated (Figures 8b,c),

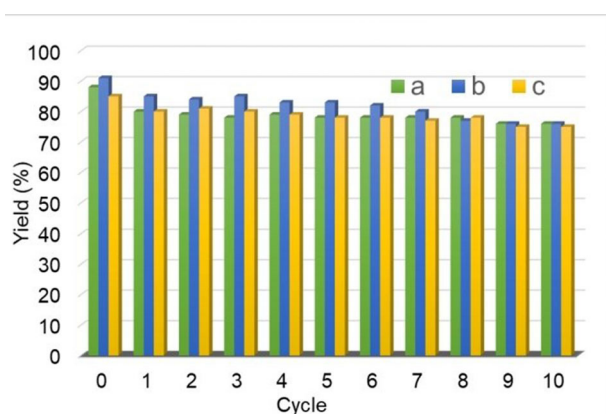


Figure 8. Reusability of PANF-NHC@Ag in the synthesis of **4a** and **4b**.

and the thermal properties of the fibers were investigated by thermogravimetry (TG) and differential scanning calorimetry (DSC; Figure S2 in the Supporting Information). In the case of PANF-NHC@Ag, it was observed that no significant degradation occurred below 200 °C. Upon decreasing the catalyst loading to 0.01% and allowing the reaction to proceed for 72 h, a 35% yield was obtained, along with an unprecedented turnover number (TON) of 3500. A mercury droplet test was conducted. The conversion did not change after the addition of mercury as a heterogeneous catalysis poison.^[11]

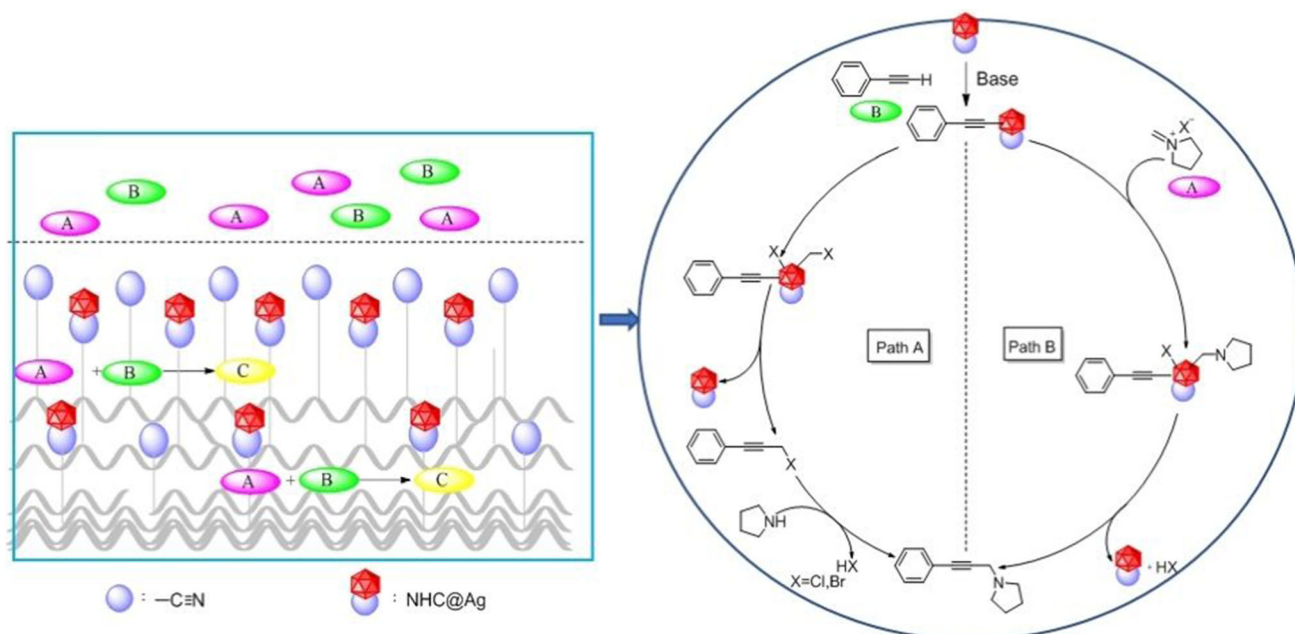
In this study, Ag particles were immobilized on the fiber surface to prevent their aggregation. Indeed, owing to the highly disperse nature and thermal stability of the AgNPs, they exhibited superior performances in the AHA reaction compared with Ag complexes and Ag salts.^[45] In addition, the incorporation of a support for the NPs inhibited particle growth and aggregation,^[1,5] with the modified PANF promoting NP generation while also protecting against aggregation. Furthermore, their adequate dispersion on the fiber surface could be attributed to chemical reduction by NaBH₄ as opposed to the use of traditional thermal decomposition methods during NP formation. Moreover, the NHC moieties act as protecting groups to prevent aggregation of the fine AgNPs.^[9,13] It should also be noted that a low yield was obtained when PANF-Am@Ag was employed as the catalyst in this transformation (Table S3 in the Supporting Information, entry 2).

Catalytic mechanism of the supported catalysts in the three-component coupling reaction

A plausible reaction mechanism for the PANF-NHC@Ag-catalyzed AHA reaction is outlined in Scheme 2, where two potential pathways are suggested. In path A, the dihalomethane substrate interacts with the metal-alkynyl complex to give a propargylhalide intermediate, which further interacts with the amine substrate to yield the desired product. In path B, the dihalomethane interacts with the amine to produce an iminium ion intermediate, which reacts with the metal-alkynyl complex to afford the desired product. Indeed, previous literature suggested that path A dominates in copper-catalyzed reactions,^[39] whereas path B dominates in iron-^[43] and gold-^[37]-catalyzed reactions. Based on these reports and on our experimental results, the three-component coupling reaction was considered to follow path B. According to this mechanism, methaniminium chloride is initially formed by the reaction of the amine with CH₂Cl₂. The corresponding propargylamine can then be obtained quantitatively from this isolated intermediate^[45] through its reaction with the silver acetylide.

Flow chemistry

Continuous-flow microreactors and their application in chemical syntheses can be considered an effective alternative strategy to conventional batch-based regimes.^[50-53] With the above promising results in hand, the high stability (Figure S2 in the Supporting Information) and excellent catalytic activity exhibited by PANF-NHC@Ag indicate its potential as a suitable cata-



Scheme 2. Proposed mechanism for the AgNP-catalyzed AHA reaction.

lyst for application in continuous-flow processes. Thus, in the context of this study, we employed an experimental setup consisting of a silicone column (100 mm length, 4.6 mm inner diameter) and a peristaltic pump (Figure 9). The fiber was cooled

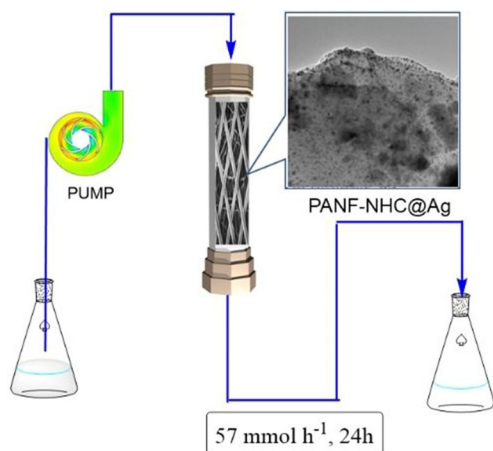


Figure 9. Schematic representation of the continuous-flow process.

with liquid nitrogen and ground into particles of approximately 1–5 μm diameter. The silicone column was operated with a PANF-NHC@Ag loading of 1.0 g (functionality = 0.75 mmol g^{-1}). A stock solution containing the substituted alkyne **1** (1.0 mol), dihalomethane **2** (5 mol), amine **3** (1.2 mol), and DBU (1.0 mol) was pumped into the continuous-flow device at 25°C , with an optimized flow rate of 0.5 mL min^{-1} giving a yield of 95%. The retention time for this reaction was 3.3 min and a productivity of **4a** of 57 mmol h^{-1} was achieved. In addition, the experiment time was set at 24 h when the reagent solution was continuously injected into the system. This resulted in an instant

yield of $>85\%$ at the end of this period. Furthermore, waste production was notably minimized by this flow process, and a long catalyst life time of 24 h was achieved as a result of minimal exposure to air or humidity.^[52] In comparison with other reported catalytic systems for the AHA reaction, PANF-NHC@Ag is superior because of its high catalytic activity, its excellent reusability, and its suitability for application in the absence of solvent (Table 2).

Table 2. Different catalytic systems for the AHA coupling reaction.				
Catalyst	$T [^\circ\text{C}]/t [\text{h}]$	Solvent	Reusability	Ref.
AuNPs	50/24	CH_2Cl_2	–	37
CuCl	25/36	CH_3CN	–	38
CuCl	60/24	CH_3CN	–	39
CuI	80/18	CH_3CN	–	41
nano In_2O_3	65/16	DMSO	3	42
FeCl_3	100/12	CH_3CN	–	43
CoBr_2	80/24	CH_3CN	–	44
AgOAc	120/12	dioxane	–	45
Au/CeO_2	65/24	CH_3CN	3	46
PANF-NHC@Ag	25/2	neat	10	this work

Conclusions

We herein reported the preparation and characterization of N-heterocyclic carbene (NHC)-stabilized silver nanoparticles (NPs) supported on polyacrylonitrile fiber (PANF) and the subsequent application of the immobilized NPs as catalysts for the efficient synthesis of propargylamines. The particle size of the AgNPs was successfully tuned by varying the functionalities and the reduction time to yield AgNPs with a loading of 8% and an average diameter of $11.0 \pm 3.2 \text{ nm}$. Essentially, the cooperative effect between the PANF support and the NHC ligand stabi-

lized the AgNPs to prevent aggregation, and the resulting PANF-NHC@Ag catalyst exhibited a high activity for the three-component reaction between aldehydes, halomethanes, and alkynes (AHA coupling), which proceeded smoothly in the absence of solvents. Furthermore, the PANF-NHC@Ag catalyst particles could be easily recovered by simple filtration and were reusable over eight cycles. Under the reaction conditions employed, the AgNP catalyst exhibited no loss in activity and no leaching of Ag into the reaction solution was observed. These observations are of particular importance as they led to the development of a stabilized metal NP catalyst system suitable for application in continuous-flow processes.

Experimental Section

General experimental information (materials, characterization, and measurements), characterization of the products, and additional tables and figures are provided in the Supporting Information.

Typical procedure for preparation of PANF-NHC-Ag

Dried PANF (5.0 g), deionized water (50 mL), and ethylenediamine (100 mL) was introduced into a 250 mL three-neck flask. The suspension was heated to reflux for 2 h. Next, the modified PANF was filtered out and washed with deionized water at 70–80 °C until the pH of the washed water was 7. Then, the modified fiber was dried overnight under vacuum at 60 °C to give the aminated PANF. The weight gain of aminated PANF was 16.2% (functionality: 2.1 mmol g⁻¹).

The NHC-Ag complex ([N-benzyl-N'-(methoxycarbonyl methyl)imidazolin-2-ylidene]silver chloride) was prepared as described in the Supporting Information. To a solution of NHC-Ag complex (3.2 g, 9.5 mmol) in CH₃CN (75 mL), ethylenediamine-aminated PANF (2.0 g, functionality: 2.1 mmol g⁻¹) was added, and the suspension was stirred at reflux for 4 h. The modified fiber was then filtered and washed with CH₃CN in a Soxhlet extractor for 24 h. Then, the modified fiber was dried under vacuum to give PANF-NHC-Ag (2.7 g, weight gain: 35%, Ag carbene functionality: 0.75 mmol g⁻¹). The functionalities of PANF can be tuned by feed ratio and reaction time (Table S1 in the Supporting Information).

Typical procedure for preparation of PANF-NHC@Ag

A mixture of PANF-NHC-Ag (1.3 g, functionality: 0.75 mmol g⁻¹) and NaOH (0.2 g) were added to deionized water (10 mL). Then, aqueous NaBH₄ solution (100 mL, 0.1 M) was added under vigorous stirring. The reaction mixture was stirred for 6 h. The modified fiber was filtered out and washed with deionized water and EtOH, then dried under vacuum at 60 °C for 12 h to afford the PANF-NHC@Ag (1.2 g).

General procedure of the AHA reaction catalyzed by PANF-NHC@Ag

Under a nitrogen atmosphere, the PANF-NHC@Ag catalyst (26 mg, containing Ag 0.01 mmol), alkyne **1** (1.0 mmol, 1.0 equiv), haloalkane **2** (1.2 mmol, 1.2 equiv), amine **3** (1.2 mmol, 1.2 equiv), and DBU (2.0 mmol) were added to a three-neck flask. The mixture was stirred at 25 °C for 3 h. After the reaction was completed as indicated by thin layer chromatography (TLC), the reaction mixture was filtered. The catalyst was washed with CH₃CN for recycling. The combined organics were then concentrated, and the residue was

purified by flash chromatography on silica gel (eluent: hexane/ethyl acetate = 4:1, v/v) to give the corresponding propargylamine.

Acknowledgments

This work was supported by the innovation team funding (1649) from the Institute of Radiation Medicine, Chinese Academy of Medical Sciences & Peking Union Medical College, the Fundamental Research Fund for CAMS&PUMC (2016ZX310199), the CAMS Innovation Fund for Medical Science (CIFMS, 2017-I2M-3-019) from the Chinese Academy of Medical Sciences & Peking Union Medical College, and Tianjin Major Scientific and Technological Special Project for Significant New Drugs Developments (17ZXXYSY00090).

Conflict of interest

The authors declare no conflict of interest.

- [1] R. J. White, R. Luque, V. L. Budarin, J. H. Clark, D. J. Macquarrie, *Chem. Soc. Rev.* **2009**, *38*, 481.
- [2] L. Rizzello, P. P. Pompa, *Chem. Soc. Rev.* **2014**, *43*, 1501.
- [3] X. Hu, S. Dong, *J. Mater. Chem.* **2008**, *18*, 1279.
- [4] F. Meemken, A. Baiker, *Chem. Rev.* **2017**, *117*, 11522.
- [5] P. Munnik, P. E. de Jongh, K. P. de Jong, *Chem. Rev.* **2015**, *115*, 6687.
- [6] Y. Sun, *Chem. Soc. Rev.* **2013**, *42*, 2497.
- [7] B. L. Cushing, V. L. Kolesnichenko, C. J. O'Connor, *Chem. Rev.* **2004**, *104*, 3893.
- [8] L. S. Ott, R. G. Finke, *Coord. Chem. Rev.* **2007**, *251*, 1075.
- [9] M. J. MacLeod, J. A. Johnson, *J. Am. Chem. Soc.* **2015**, *137*, 7974.
- [10] N. Möller, A. Ruehling, S. Lamping, T. Hellwig, C. Fallnich, B. J. Ravoo, F. Glorius, *Angew. Chem. Int. Ed.* **2017**, *56*, 4356; *Angew. Chem.* **2017**, *129*, 4421.
- [11] A. Rühling, K. Schaepe, L. Rakers, B. Vonhören, P. Tegeder, B. J. Ravoo, F. Glorius, *Angew. Chem. Int. Ed.* **2016**, *55*, 5856; *Angew. Chem.* **2016**, *128*, 5950.
- [12] K. V. S. Ranganath, J. Kloesges, A. H. Schäfer, F. Glorius, *Angew. Chem. Int. Ed.* **2010**, *49*, 7786; *Angew. Chem.* **2010**, *122*, 7952.
- [13] K. Salorinne, R. W. Y. Man, M. Taki, M. Nambo, C. M. Crudden, C.-H. Li, C. M. Crudden, *Angew. Chem. Int. Ed.* **2017**, *56*, 6198; *Angew. Chem.* **2017**, *129*, 6294.
- [14] A. Ferry, K. Schaepe, P. Tegeder, C. Richter, K. M. Chepiga, B. J. Ravoo, F. Glorius, *ACS Catal.* **2015**, *5*, 5414.
- [15] J. B. Ernst, S. Muratsugu, F. Wang, M. Tada, F. Glorius, *J. Am. Chem. Soc.* **2016**, *138*, 10718.
- [16] V. K. Sharma, R. A. Yngard, Y. Lin, *Adv. Colloid Interface Sci.* **2009**, *145*, 83.
- [17] M. A. Bhosale, B. M. Bhanage, *Curr. Org. Chem.* **2015**, *19*, 708.
- [18] X.-Y. Dong, Z.-W. Gao, K.-F. Yang, W.-Q. Zhang, L.-W. Xu, *Catal. Sci. Technol.* **2015**, *5*, 2554.
- [19] D. Yu, M. X. Tan, Y. Zhang, *Adv. Synth. Catal.* **2012**, *354*, 969.
- [20] H. E. Emam, M. M. El-Zawahry, H. B. Ahmed, *Carbohydr. Polym.* **2017**, *166*, 1.
- [21] G.-P. Yong, D. Tian, H.-W. Tong, S.-M. Liu, *J. Mol. Catal. A: Chem.* **2010**, *323*, 40.
- [22] J.-W. Lee, T. Mayer-Gall, K. Opwis, C. E. Song, J. S. Gutmann, B. List, *Science* **2013**, *341*, 1225.
- [23] Y. Wang, R. Qu, F. Pan, X. Jia, C. Sun, C. Ji, Y. Zhang, K. An, Y. Mu, *Chem. Eng. J.* **2017**, *317*, 187.
- [24] M. Monier, I. M. Kenawy, M. A. Hashem, *Carbohydr. Polym.* **2014**, *106*, 49.
- [25] X. Xing, H. Yang, M. Tao, W. Zhang, *J. Hazard. Mater.* **2015**, *297*, 207.
- [26] D.-G. Yu, J. Zhou, N. P. Chatterton, Y. Li, J. Huang, X. Wang, *Int. J. Nanomed.* **2012**, *7*, 5725.
- [27] J. Cao, G. Xu, P. Li, M. Tao, W. Zhang, *ACS Sustainable Chem. Eng.* **2017**, *5*, 3438.
- [28] A. A. Boulton, B. A. Davis, D. A. Durden, L. E. Dyck, A. V. Juorio, X.-M. Li, I. A. Paterson, P. H. Yu, *Drug Dev. Res.* **1997**, *42*, 150.

- [29] S. Nag, G. Ketschau, T. Heinrich, A. Varrone, L. Lehmann, B. Gulyas, A. Thiele, É. Keller, C. Halldin, *Bioorg. Med. Chem.* **2013**, *21*, 186.
- [30] V. A. Peshkov, O. P. Pereshivko, E. V. Van der Eycken, *Chem. Soc. Rev.* **2012**, *41*, 3790.
- [31] Z. Dong, X. Le, X. Li, W. Zhang, C. Dong, J. Ma, *Appl. Catal. B* **2014**, *158–159*, 129.
- [32] S. M. Badawy, A. M. Dessouki, *J. Phys. Chem. B* **2003**, *107*, 11273.
- [33] C. Satheeshkumar, J.-Y. Park, D.-C. Jeong, S. G. Song, J. Lee, C. Song, *RSC Adv.* **2015**, *5*, 60892.
- [34] A. S. El-Khouly, E. Kenawy, A. A. Safaan, Y. Takahashi, Y. A. Hafiz, K. Sonomoto, T. Zendo, *Carbohydr. Polym.* **2011**, *83*, 346.
- [35] X. Liu, W. Chen, Y.-I. Hong, S. Yuan, S. Kuroki, T. Miyoshi, *Macromolecules* **2015**, *48*, 5300.
- [36] D. Erdemir, A. Y. Lee, A. S. Myerson, *Acc. Chem. Res.* **2009**, *42*, 621.
- [37] D. Aguilar, M. Contel, E. P. Urriolabeitia, *Chem. Eur. J.* **2010**, *16*, 9287.
- [38] Z. Lin, D. Yu, Y. Zhang, *Tetrahedron Lett.* **2011**, *52*, 4967.
- [39] D. Yu, Y. Zhang, *Adv. Synth. Catal.* **2011**, *353*, 163.
- [40] B. R. Buckley, A. N. Khan, H. Heaney, *Chem. Eur. J.* **2012**, *18*, 3855.
- [41] Z. Lin, D. Yu, Y. N. Sum, Y. Zhang, *ChemSusChem* **2012**, *5*, 625.
- [42] M. Rahman, A. K. Bagdi, A. Majee, A. Hajra, *Tetrahedron Lett.* **2011**, *52*, 4437.
- [43] J. Gao, Q.-W. Song, L.-N. He, Z.-Z. Yang, X.-Y. Dou, *Chem. Commun.* **2012**, *48*, 2024.
- [44] Y. Tang, T. Xiao, L. Zhou, *Tetrahedron Lett.* **2012**, *53*, 6199.
- [45] X. Chen, T. Chen, Y. Zhou, C.-T. Au, L.-B. Han, S.-F. Yin, *Org. Biomol. Chem.* **2014**, *12*, 247.
- [46] A. Berrichi, R. Bachir, M. Benabdallah, N. Choukchou-Braham, *Tetrahedron Lett.* **2015**, *56*, 1302.
- [47] M. Yu, Y. Wang, W. Sun, X. Yao, *Adv. Synth. Catal.* **2012**, *354*, 71.
- [48] V. S. Rawat, T. Bathini, S. Govardan, B. Sreedhar, *Org. Biomol. Chem.* **2014**, *12*, 6725.
- [49] Y.-B. Huang, M. Shen, X. Wang, P.-C. Shi, H. Li, R. Cao, *J. Catal.* **2015**, *330*, 452.
- [50] J. C. Pastre, D. L. Browne, S. V. Ley, *Chem. Soc. Rev.* **2013**, *42*, 8849.
- [51] J. Britton, C. L. Raston, *Chem. Soc. Rev.* **2017**, *46*, 1250.
- [52] D. Cambié, C. Bottecchia, N. J. W. Straathof, V. Hessel, T. Noël, *Chem. Rev.* **2016**, *116*, 10276.
- [53] M. B. Plutschack, B. Pieber, K. Gilmore, P. H. Seeberger, *Chem. Rev.* **2017**, *117*, 11796.

Manuscript received: January 29, 2018

Revised manuscript received: April 2, 2018

Version of record online: ■ ■ ■, 0000

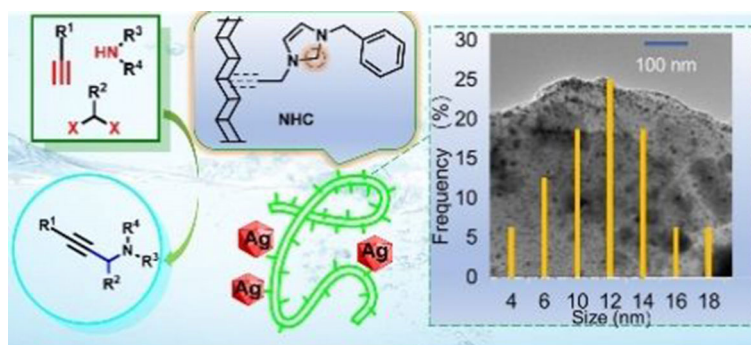
FULL PAPER

Three-Component Coupling Reaction

Jian Cao, Hongqi Tian*

■■ - ■■

 **N-Heterocyclic Carbene-Protected Ag Nanoparticles Immobilized on Polyacrylonitrile Fiber as Efficient Catalysts for a Three-Component Coupling Reaction**



Carbenes for coupling: N-heterocyclic carbene (NHC)-stabilized silver nanoparticles (NPs) supported on polyacrylonitrile fiber (PANF). As a result, Ag loadings of up to 8% and particle sizes of 11.0 ± 3.2 nm were achieved. This novel

nanocomposite catalyst demonstrated high activity in addition to excellent stability and reusability in the three-component reaction between alkynes, haloalkanes, and amines.